Proceedings of Ninth World Conference on Earthquake Engineering
August 2-9, 1988, Tokyo-Kyoto, JAPAN (Vol.IV)

6-5-18

EXPERIMENTAL STUDY ON SEISMIC PERFORMANCE OF MULTISTORY SHEAR WALLS WITH FLANGED CROSS SECTION

Hisahiro HIRAISHI[1] Hitoshi SHIOHARA[2] Toshikazu KAWASHIMA[3]
Hiroyuki TOMATSURI[4] Akira KUROSAWA[5] Yoshiyasu BUDO[6]

[1]Head of Structure Division, Building Research Institute, Ministry of Construction, Tsukuba-shi, Ibaraki, Japan
[2]Research Associate of Structure Division, BRI, MOC, Japan
[3]Research Assistant of Structure Division, BRI, MOC, Japan
[4]Engineering Research Institute, PENTA-OCEAN Construction, Co., Ltd., Shinagawa-ku, Tokyo, Japan
[5]Mitsubishi Construction, Co., Ltd., Japan
[6]Tobishima Corporation, Co., Ltd., Japan

SUMMARY

The experimental studies showed that the final stages beyond flexural yielding of multistory shear walls were mostly determined by compressive crushing of the boundary columns and panels. Therefore, the axial compressive stress level of the boundary columns at the critical section under the yielding mechanism, was considered one of the important factors in determining the deformation capacity of multistory shear walls.

Inner beams had little effect on the load versus deflection relation, curvature distribution, and shear and flexural deformations.

INTRODUCTION

Reinforced concrete frame structures with wall columns have recently been developed and used in Japan. They have multistory shear walls, in the span direction, between each dwelling unit as shown in Fig. 1. Therefore, the resistance against seismic force in the span direction of the structures is governed by only the seismic performance of multistory shear walls. This paper reports the seismic performance, particularly deformation capacity, of such shear walls based on the test results of 5 shear wall specimens of a 1/4 scale model, representing the lower 7 stories of a 11-story prototype building. The highlights of the discussion of the test in this paper are : 1) the effect of the boundary columns (the axial compressive stress level of the boundary column at the critical section on the deformation capacity of multistory shear walls), and 2) the effects of inner beams on deformation characteristics.

TEST SPECIMENS AND TEST PROCEDURE

The properties of the specimens are listed in Table 1. The specimens were designed to yield in flexure before they reached shear strength. Figure 2 shows the layout of reinforcement used in Specimen WF-2. The controlled variable included in Specimens WF-2, WF-3, and WF-4 was the sectional area of the boundary columns as shown in Fig. 3. Specimen WF-1 was the same as WF-2 except for having inner beams. Specimen WF-5 had heavy confining reinforcement, in boundary columns, and a thicker wall panel (1.33 times that of the other specimens). The shear reinforcement in the panel wall in lateral direction was provided so that the shear strength exceeded the flexural strength.

Material For the concrete, ordinary portland cement and normal weight aggregate with the maximum size of 10mm were used. Table 2 gives strengths of the concrete used in the specimens. Table 3 gives mechanical properties of reinforcing steels.

The testing setup is shown in Fig. 4. The lateral force was applied to the top of the specimen. The specimen was also subjected to the axial load, in addition to the self weight of the specimens, in order to simulate the axial stress acting on the first story of the 11-story prototype building. The loading was controlled by the drift angle (R_1) of the first story. The loading history is shown in Fig. 5.

TEST RESULTS

Attained maximum loads and ultimate deflections of the tests are listed in Table 4. The envelope curves of the load versus drift relations of the first story and fourth-story are shown in Figs. 6 and 7, respectively. Figure 8 shows the load versus drift angle hysteresis (R_4) and its envelope (R_1) curve. Observed appearances of specimens after tests are shown in Fig. 9.

A similar sequence of crack occurrence was observed in the specimens except for Specimen WF-5 until the loading cycle of R_1=1/200 rad. In the loading cycle of R_1=1/400 rad, shear cracks occurred in the wall panel of each story. Almost all longitudinal reinfocing bars yielded at the base of the wall panel in this cycle.

Specimen WF-1 The beams somewhat prevented development of cracking of the wall panel. In the loading cycle of R_1=1/67 rad, compressive crushing of concrete began at the corner of the wall panel of the first story. In the loading cycle of R_1=1/50 rad, cover concrete crushed at the base of columns, and vertical reinforcing bars at the base of the wall panel buckled. In this cycle, the lateral load decreased to 80% of the maximum strength. Thereafter the specimen maintained the load against the further increment of deflection, and compressive crushing of concrete occurred around the base of the wall panel.

Specimen WF-2 In the loading cycle of R_1=1/100 rad, compressive crushing of concrete occurred at the base of the wall panel. In the next loading cycle of R_1=1/67 rad, vertical reinforcing bars in the wall panel buckled, and compressive crushing of concrete began at the base of the columns. But the area of compressive crushing of concrete of the columns scarcely extended thereafter. The failure concentrated in the wall panel near the boundary columns under compression without rapid deterioration in strength.

Specimen WF-3 In the loading cycle of R_1=1/100 rad, crushing of the cover concrete began at the critical section of the boundary columns. In the next loading cycle of R_1=1/67 rad, web crushing occurred along the boundary columns and reinforcing bars in wall panel buckled. In loading cycle of R_1=1/50 rad, longitudinal reinforcing bars in the columns buckled. Thereafter, web crushing extended for larger deflection and the lateral load gradually reduced.

Specimens WF-4 and WF-5 The sequence of crack occurrence in Specimens WF-4 and WF-5 were similar each other. In the loading cycle of R_1=1/100 rad, crushing of the cover concrete of the column was observed. In the next loading cycle, web crushing also began. In the final stage of the test, reinforcing bars in the wall panel and the main reinforcing bars in the columns buckled and concrete in the compressive zone crushed completely. Due to this failure mode, the lateral load carrying capacity decreased rapidly in Specimen WF-4 while such deterioration in strength was not observed in Specimen WF-5 whose wall thickness was thicker than that of Specimen WF-4. The number of cracks observed in Specimen WF-5 was less than those of the other specimens. The deformation capacity of Specimen WF-5, having the thicker wall panel and heavy confining reinforcement in the boundary column, is much better than that of Specimen WF-4.

DISCUSSION OF DEFORMATION CAPACITY

The Axial Compressive Stress Level of the Boundary Column Figure 10 shows the equilibrium of the forces and moment at the base of shear wall at hinge mechanism. For simplicity, only the column in the compression side is assumed to be subjected to compressive force at the base (see Fig. 11). Thus, the compressive force (C_c) of the boundary column at the compression side is given by the following equation:

$$C_c = T_s + T_w + N, \quad T_s = a_t \cdot \sigma_y, \quad T_w = a_{wy} \cdot \sigma_{wy} \tag{1}$$

where T_s and T_w = the tensile forces in longitudinal reinforcing bars in the column and wall panel, respectively; N = the axial force; a_t = the sectional area of longitudinal reinforcing bars in column under tension; σ_y = the yield strength of reinforcing bars in column; a_{wy} = the cross sectional area of reinforcing bars in wall panel, and σ_{wy} = the yield strength of reinforcing bar in wall panel.

The compressive strength (C_D) of column is given by Eq.(2) :

$$C_D = bD\sigma_B + a_c \cdot \sigma_y \tag{2}$$

where a_c = the cross sectional area of longitudinal reinforcing bars in column under compression; and b,D = the width and depth of the column, respectively. Hereafter, the axial compressive stress level (η_c) of boundary column is defined by Eq.(3) :

$$\eta_c = C_c / C_D = (T_s + T_w + N)/(bD\sigma_B + a_c \cdot \sigma_y) \tag{3}$$

Factors Affecting on Deformation Capacity Factors which may influence the deformation capacity of multistory shear walls were investigated based on the test results together with past test results of shear walls[1] (22 specimens) satisfying the following conditions : a) flexural yielding prior to shear failure, b) shear span ratio more than 1.2, c) cantilever type loading system, d) isolated shear wall, and e) shear wall without opening. The descriptions related to the final stages of these test results are as follows : 1) Crushing of column (11 specimens), 2) Web crushing (13 specimens), 3) Buckling of longitudinal reinforcing bars in column (3 specimens), 4) Slipping failure of wall panel (3 specimens), and 5) Shear failure in column (2 specimens). That is to say, the major cause of the final stages of multistory shear walls was concrete crushing of the columns and wall panel.

Figures from 12 to 15 show the relationships between the deformation capacity and each factor (Q_{su}/Q_{mu}, τ_u/σ_B, η_c, and Q_w/Q_{mu}) which are considered to have influence on deformation capacity of shear walls. Here, the deformation capacity (R_u) was defined as the deformation at 80% of the maximum strength. Marks (○) in these figures denote the specimens whose value of Q_{su}/Q_{mu} was below 1.0. From the plot in Fig. 12, the deformation capacity is estimated to be more than 1×10^{-2}rad. approximately, if the value of Q_{su}/Q_{mu} is greater than 1.0. But no clear relation exists between R_u and Q_{su}/Q_{mu} or R_u and τ_u/σ_B, if the marks representing the specimens whose values of Q_{su}/Q_{mu} were less than 1.0 are omitted. On the contrary, Ru decreases as the ratio (η_c) becomes larger. Therefore, it is important for the design of ductile shear walls that the axial compressive stress level (η_c) is controlled within a certain low value.

EFFECTS OF BEAMS

Stiffness at Yielding The envelope curves of Specimens WF-1 (with beams) and WF-2 (without beams), are compared in Fig. 16. At R_1=1/800 rad, when longitudinal reinforcing bars in columns reached their yield strains, Specimen WF-1 had higher stiffness than Specimen WF-2.

Distribution of Curvature Figure 17 shows the curvature distributions of Specimens WF-1 and WF-2 at R_1=1/200, 1/100, and 1/67 radians. The curvature distributions of Specimen WF-1 shows some irregularity around beams, however, the curvature distributions of each specimens is approximated by a parabolic line

macroscopically.

Shear And Flexural Deformations Figure 18 shows the relationships between the drift angle R_4 versus shear and flexural deformations of Specimens WF-1, WF-2, and WF-3. Figure 18 shows the analytical values which were estimated from the theory reported in Ref. 2. Longitudinal bars in the beams were taken into account as the horizontal shear reinforcement in wall panel. However, there was no remarkable difference in the deformation components between Specimen WF-1 and the others, because the amount of total horizontal reinforcement was almost the same (equivalent horizontal reinforcement ratio is 0.533 for Specimen WF-2 and 0.686 for the others). The theoretical results agreed excellently with the test ones.

Deformation Capacity As referred to in the preceding chapter, the deformation capacity of Specimen WF-2 was not less than that of Specimen WF-1 with beams.

CONCLUSIONS

1) The ratio (η_c) should be smaller than about 0.7 so that the multistory shear walls might behave in an excellent ductile manner.
2) The factors such as Q_{su}/Q_{mu}, τ_u/σ_B, and Q_w/Q_{mu} do not influence on the deformation capacity of multistory shear walls if their minimum requirements are satisfied.
3) The deformation capacity of Specimen WF-2 without beams was not less than that of Specimen WF-1 with beams. The Specimen WF-1 had the higher stiffness at yielding.
4) The deformation capacity can be improved by arranging heavy confining reinforcement in the boundary column and by making the wall panel thicker.

REFERENCES

1. Hiraishi, H., "The Deformation Capacity of Multistory Shear Walls," Symposium of Architectural Institute of Japan, Kanto Branch, 1986. (in Japanese)
2. Hiraishi, H., "Analytical Study on Load vs. Deformation Relationship of Flexural Type Reinforced Concrete Shear Walls," Journal of Structural and Construction Engineering, AIJ, No.347, 95-101, 1985. (in Japanese)
3. Hiraishi, H., "An Evaluation Method for Shear and Flexural Deformations of Shear Walls," Journal of Structural and Construction Engineering, AIJ, No.333, 55-62, 1983. (in Japanese)

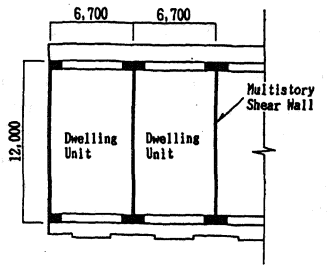

Fig.1 Plan of a R/C Frame Structure with Wall Columns

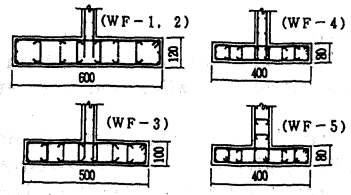

Fig.3 Cross Sections of Specimens

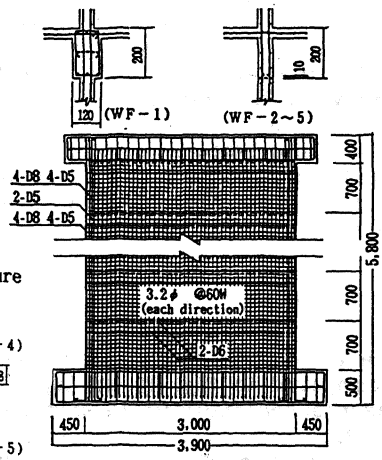

Fig.2 Specimen(WF-2)

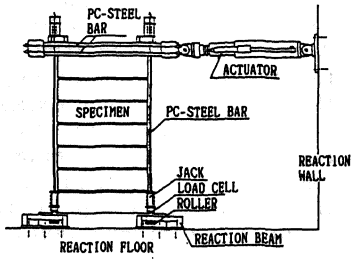

Fig.4 Test Set-up

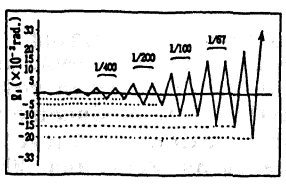

Fig.5 Deflection History

Table 1 Specimens and Design Values of Variables

(Common : σ_B =240 kg/cm², σ_y =3850 kg/cm², σ_{wy} =3300 kg/cm²)

Name	Factors of Test: η_c [1]	Beams in Wall Panel	Reinforcement in Columns	Column: b×D(cm) σ_0 [2] p_g [3] (%) p_w [4] (%)	Beam: b×D(cm) Main Bar p_w(%)	Wall Panel: t×ℓ_w(cm) Reinforcement p_{sv}, p_{sh} [5] (%)	Predicted: Qsu/Qmu [6] Qw /Qmu [7] M /QD	Failure Mode τ_u [8] τ_u /σ_B
WF-1	0.6	with beams	confined with sub-tie	12×60 21.3 0.82 0.84 0.41	12×20 3-D6,3-D6 0.2	6×288 Longitudinal φ3.2@60D Lateral φ3.2@60D 0.447 0.447	1.41 1.06 0.48 1.70	Flexure 22.23 0.093
WF-2	0.6	without beams						
WF-3	0.8	without beams		10×50 24.6 1.18 1.01 0.48	2-D6,2-D6	6×290 Longi.ditto Lateral φ3.2@50D 0.447 0.536	1.39 1.07 0.50 1.70	Flexure 22.23 0.093
WF-4	1.1	without beams		8×40 28.2 1.85 1.26 0.71		6×292 Longi.ditto Lateral φ3.2@45D 0.447 0.596	1.36 1.05 0.51 1.70	Flexure 22.31 0.093
WF-5	1.1	without beams	confined with sub-hoops at center and both sides	8×40 22.7 1.85 1.26 0.71		8×292 Longi.ditto Lateral φ3.2@45D 0.335 0.447	1.59 1.22 0.58 1.70	Flexure 16.73 0.070

Notes 1) The ratio (η_c) of assumed compressive force in column (see Fig.19) at the critical section at maximum strength to compressive strength of column ; η_c is giving by the following equation.
$\eta_c = C_c/C_B = (\Sigma a_t \sigma_y + \Sigma a_w \sigma_{wy} + \Sigma N)/(b D \sigma_B + \Sigma a_c \sigma_y)$

2) σ_0 : axial stress for whole cross sectional area (kg/cm²) $\sigma_0 = N/(\Sigma A_c + A_w)$

A_c : cross sectional area of column (cm²), A_w : cross sectional area of wall panel (cm²)

3) p_g : ratio of total sectional area of longitudinal reinforcing area to 'A_c'

4) p_w : reinforcement ratio of hoops of column
Value at left hand side represents 'p_w' in span direction and the other does 'p_w' in ridge direction.

5) p_{sv} : shear reinforcement ratio in horizontal direction in wall panel
p_{sh} : shear reinforcement ratio in vertical direction in wall panel

6) Qsu/Qmu : ratio of shear strength to flexural one
value at left hand side : $Qsu = (0.0679 p_{te}^{0.23}(Fc+180)/\sqrt{(M/QD+0.12)} + 2.7\sqrt{p_{sw}\sigma_{wy}} + 0.1\sigma_0) b_e \cdot j$ (kg)
value at right hand side : $Qsu = (0.053 p_{te}^{0.23}(Fc+180)/(M/QD+0.12) + 2.7\sqrt{p_{sw}\sigma_{wy}} + 0.1\sigma_0) b_e \cdot j$ (kg)
where, 'b_e' is equal to '(t+2b)', if 'D' is greater than '(t+2b)'.
$Qmu = (\Sigma a_t \sigma_y + 0.5\Sigma a_w \sigma_{wy} + 0.5N)\ell_w/a$ (kg) , a : shear span = 510 (cm)

7) $Qw = 2.7\sqrt{p_{sw} \cdot \sigma_{wy}}\ be \cdot j$ (kg)

8) τ_u : shear stress = $Qmu/(t \times \ell_w)$ (kg/cm²)
t : wall thickness (cm), ℓ_w : column center to column center length (cm)

Table 2 Concrete Properties

Specimen	Compressive Strength σ_B (kg/cm²)	Strain at σ_B ε_{max} (%)	Young's Modulus E_c (×10³kg/cm²)
WF-1	237	0.22	2.13
WF-2	252	0.22	2.04
WF-3	205	0.20	1.83
WF-4	292	0.22	2.34
WF-5	224	0.21	1.96

Table 3 Reinforcement Properties

Size Designation	Sectional Area a_t (cm²)	Yield σ_y (kg/cm²)	Strength σ_u (kg/cm²)	Young's Modulus E_c (×10³ kg/cm²)
D 8	0.500	4207	6111	2.10
D 6	0.320	3792	5849	1.66
D 5	0.196	3207	4785	2.01
D 4	0.125	2793	4414	1.94
4.0φ	0.126	2834	4447	1.92
3.2φ	0.080	2763	4452	1.94
3.0φ	0.071	2543	5936	1.97
2.6φ	0.053	2637	4412	1.76

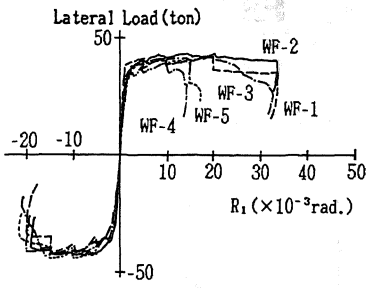

Fig.6 Load versus Drift Angle Envelopes (1st-story)

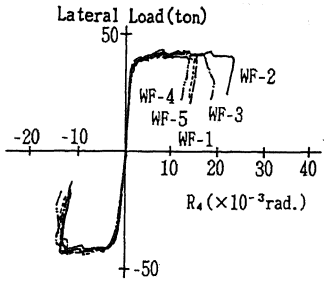

Fig.7 Load versus Deflection Envelopes (4th-story)

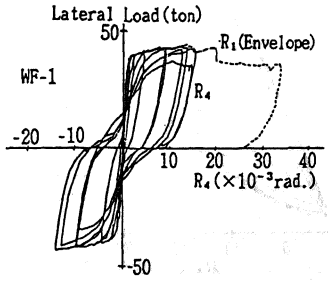

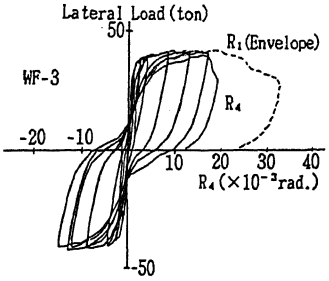

Fig.8 Load versus Drift Angle (R_4) Hysteresis and Envelope (R_1)

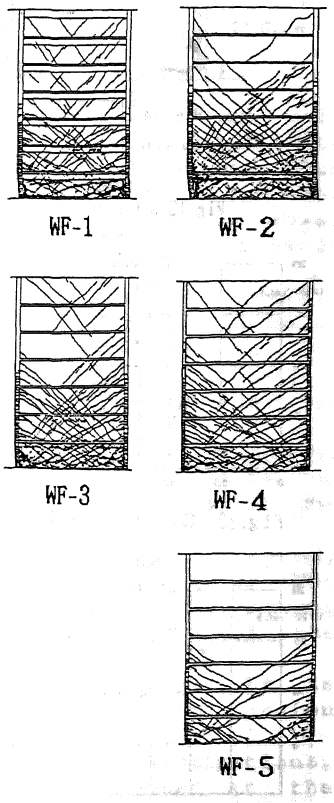

Fig.9 Specimens After Testing

Table 4 Test Results

Specimen		η_c	At Maximum Lateral Load				At Ultimate Deflection*1			Measured and Calculated			
			Q_{max} (ton)	τ_{max} / τ_{max}/F_c	δ_1 R_1	δ_4 R_4	Q_u (ton)	δ_1 R_1	δ_4 R_4	Q_{mu1} (ton)	Q_{max}/Q_{mu1}	Q_{mu2} (ton)	Q_{max}/Q_{mu2}
WF-1	P	0.57	43.1	24.9 0.105	8.04 (13.4)	31.82 (11.8)	41.9	12.04 (20.1)	41.03 (15.2)	37.6	1.15	36.2	1.19
	N		43.8	25.3 0.107	9.03 (15.1)	37.89 (14.0)	——	——	——		1.16		1.21
WF-2	P	0.54	43.4	25.1 0.100	5.09 (8.5)	20.19 (7.5)	39.9	20.02 (33.4)	61.94 (22.9)		1.15	36.3	1.20
	N		43.2	25.0 0.099	4.25 (7.1)	17.51 (6.5)	——	——	——		1.15		1.19
WF-3	P	0.87	41.6	23.9 0.117	11.22 (18.7)	42.24 (15.6)	41.0	12.03 (20.1)	45.22 (16.7)	37.8	1.10	36.1	1.15
	N		42.2	24.3 0.118	8.96 (14.9)	34.05 (12.6)	——	——	——		1.12		1.17
WF-4	P	0.94	40.3	23.0 0.079	4.84 (8.1)	18.64 (6.9)	39.0	8.96 (14.9)	36.76 (13.6)	38.1	1.06	36.2	1.11
	N		43.0	24.5 0.084	5.91 (9.9)	25.64 (9.5)	——	——	——		1.13		1.19
WF-5	P	1.16	40.3	17.3 0.077	7.74 (12.9)	34.40 (12.7)	39.2	8.92 (14.9)	39.68 (14.7)		1.06	36.1	1.12
	N		44.2	18.9 0.084	8.95 (14.9)	33.50 (12.4)	——	——	——		1.16		1.22

Notes η_c : the value of giving by Eq.(6) putting into actual material properties.
δ_1, δ_4 : displacement of 1st-story and 4th-story (mm)
R_1, R_4 : drift angle of 1st-story and 4th-story ($\times 10^{-3}$rad.)
$R_1 = \delta_1/h_1$ (h_1=600mm), $R_4 = \delta_4/h_2$ (h_2=2700mm)
$\tau_{max} = Q_{max} / t \times \ell_w$
$Q_{mu1} = \{\Sigma a_t \sigma_y + 0.5 \Sigma a_{wy} \sigma_{wy} + 0.5 N\} \ell_w/a$
$Q_{mu2} = \{0.9\Sigma a_t \sigma_y + 0.4 \Sigma a_{wy} \sigma_{wy} + 0.5 N (1-\sigma_0/F_c)\} D/a$
*1 : the value at larger displacement at descending of 80% at the maximum.
P : possitive loading N : negative loading

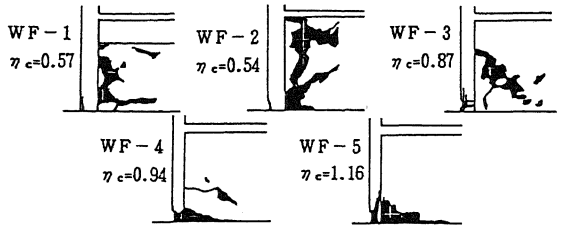

Fig.10 Schematic Views of Failure of Concrete

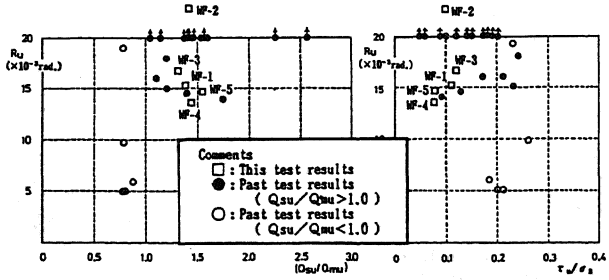

Fig.12 Q_{su}/Q_{mu} versus R_u

Fig.13 τ_u/σ_B versus R_u

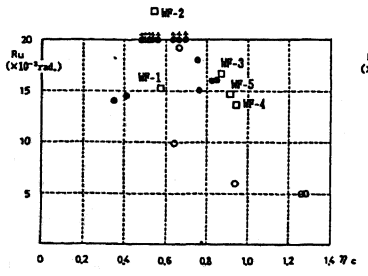

Fig.14 η_c versus R_u

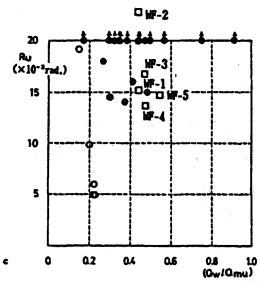

Fig.15 Q_w/Q_{mu} versus R_u

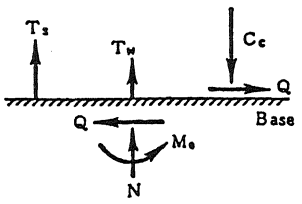

Fig.11 Forces and Moments at the Base

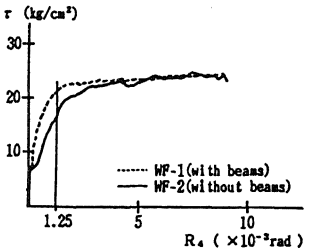

Fig.16 Load versus Deflection (WF-1, WF-2)

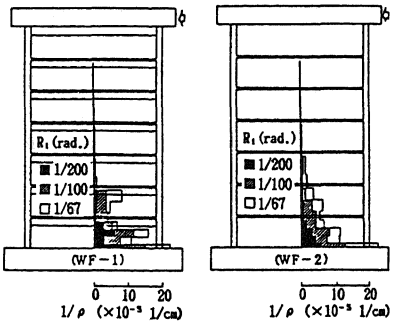

Fig.17 Curvature Distribution

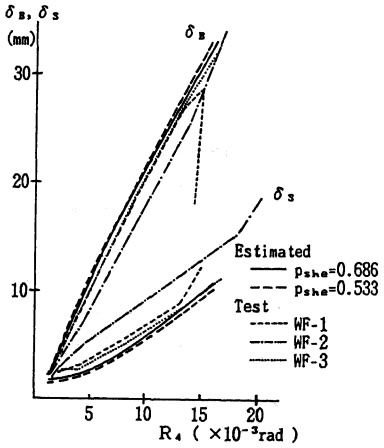

Fig.18 Distribution of Flexural and Shear Deformations